Journal of Civil and Hydraulic Engineering
https://www.acadlore.com/journals/JCHE

Numerical Simulation of Resistivity Response Characteristics in Seepage Detection of Cutoff Walls Using Cross-Hole Resistivity Tomography

Qicheng Fu[1,2,3], Xinjiang Yu[1,2,3], Bo Li[1,2,3*], Junjie Zhou[4], Shiwen Fan[4], Shengbo Mei[4], Lingzhi Li[1,2,3]

[1] Changjiang River Scientific Research Institute, 430010 Wuhan, China
[2] Engineering Safety and Disaster Prevention Department, Changjiang River Scientific Research Institute, 430010 Wuhan, China
[3] National Dam Safety Engineering Technology Research Center, 430010 Wuhan, China
[4] Shanxi Datong Pumped Storage Co., Ltd., 037400 Datong, China

[*] Correspondence: Bo Li (lb007403@163.com)

Received: 08-26-2024 **Revised:** 09-28-2024 **Accepted:** 10-10-2024

Citation: Q. C. Fu, X. J. Yu, B. Li, J. J. Zhou, S. W. Fan, S. B. Mei, and L. Z. Li, "Numerical simulation of resistivity response characteristics in seepage detection of cutoff walls using cross-hole resistivity tomography," *J. Civ. Hydraul. Eng.*, vol. 3, no. 1, pp. 8–16, 2025. https://doi.org/10.56578/jche030102.

Abstract: Cutoff walls are an essential method for seepage prevention in dams. During the construction and operation of reservoirs, factors such as construction techniques, variations in groundwater conditions within the dam body, geological movements, and climatic factors may lead to potential seepage risks, necessitating inspection. Traditional methods like borehole coring and water pressure tests have limited monitoring ranges, while non-destructive methods like high-density electrical surveys and shallow seismic exploration have low deep-resolution capabilities, making them unsuitable for detecting deep-seated seepage in concrete walls. In recent years, Cross-borehole Tomography (CT) geophysical techniques, based on boreholes on both sides, have been widely applied in various engineering geophysical projects. Seepage in cutoff walls can lead to an increase in local moisture content, resulting in low-resistivity anomalies, providing a physical basis for the exploration using cross-borehole resistivity CT. This study investigates the resistivity response characteristics of cross-borehole resistivity CT through numerical simulation based on the resistivity characteristics of seepage in cutoff walls. The numerical simulation results indicate that this method effectively identifies seepage conditions in cutoff walls, and the resolution of cross-borehole resistivity CT is significantly related to the cross-hole spacing and the distance to the seepage points. This study provides a preliminary verification of the feasibility of applying cross-borehole resistivity CT for detecting seepage in cutoff walls and offers insights for seepage detection strategies.

Keywords: Cutoff wall; Cross-borehole Tomography (CT); Resistivity; Numerical simulation

1 Introduction

China has built a large number of hydraulic projects, which have played a significant role in the country's economic development. Cutoff walls are an important method for seepage prevention in dams. During the construction and operation of reservoirs, due to factors such as construction techniques, variations in groundwater conditions within the dam body, geological movements, and climatic factors, there may be potential seepage risks. Risk assessment and subsequent repair of reservoirs that may have potential hazards, and engineering inspections of reservoirs that have not been put into use, are necessary measures to eliminate safety hazards. At present, the main detection methods for cutoff walls include destructive detection methods such as core sampling and geological boreholes combined with water injection experiments [1], as well as non-destructive monitoring methods such as borehole ultrasonic television detection, high-density electrical methods, shallow seismic exploration methods, and ground-penetrating radar methods [2].

In geophysical detection methods, the resolution of high-density electrical methods decreases with increasing detection depth, and the detection depth of ground-penetrating radar and shallow seismic methods is limited. The reason for the insufficient deep resolution of the above methods is that their transmitting and receiving devices are located on the surface, too far from the detected area, making it impossible to conduct refined detection of deep

anomalies in the dam. To solve the problem of insufficient resolution for deep structure detection, cross-borehole exploration methods, which place transmitting and receiving devices on both sides of the detection area, have become an effective means to solve this problem. Currently, the CT methods used in dam hazard detection are mostly electromagnetic wave CT methods based on electromagnetic wave absorption theory and seismic wave CT methods based on elastic wave theory. Li et al. [3] used electromagnetic wave CT technology to detect the concealed weathered interface and weak interlayers of the Zuojiang dam, and the results were verified by drilling. Cao et al. [4] used the elastic wave CT method to conduct a comprehensive non-destructive detection of the dam foundation of the Qianping Reservoir, proving the feasibility of the elastic wave CT. Compared with the previous two methods, the direct current resistivity method is more sensitive to low-resistivity anomalies caused by seepage. The direct current cross-borehole resistivity CT imaging method was first proposed by Shima, inspired by medical CT, and this method was applied to geophysical work, proposing a well-to-well resistivity tomography technique for multi-directional, close-range detection of typical underground structures [5]. On the basis of previous studies, Daily and Owen [6] systematically elaborated on the direct current cross-borehole resistivity CT, providing a detailed introduction to the relevant principles of the method. At present, the cross-borehole resistivity CT method based on conductivity differences has been widely used in urban karst investigations and buried depth detection of bored piles [7, 8], while its application in hydraulic engineering is relatively rare. Seepage in cutoff walls will lead to an increase in local moisture content of the dam, resulting in low-resistivity anomaly areas, providing a physical basis for exploration using the cross-borehole resistivity CT method. To explore the feasibility of the cross-borehole resistivity CT method in dam seepage detection, this paper uses forward numerical simulation and inversion of synthetic data to study the apparent resistivity response characteristics of cross-borehole resistivity CT before and after seepage in cutoff walls.

2 Method Overview

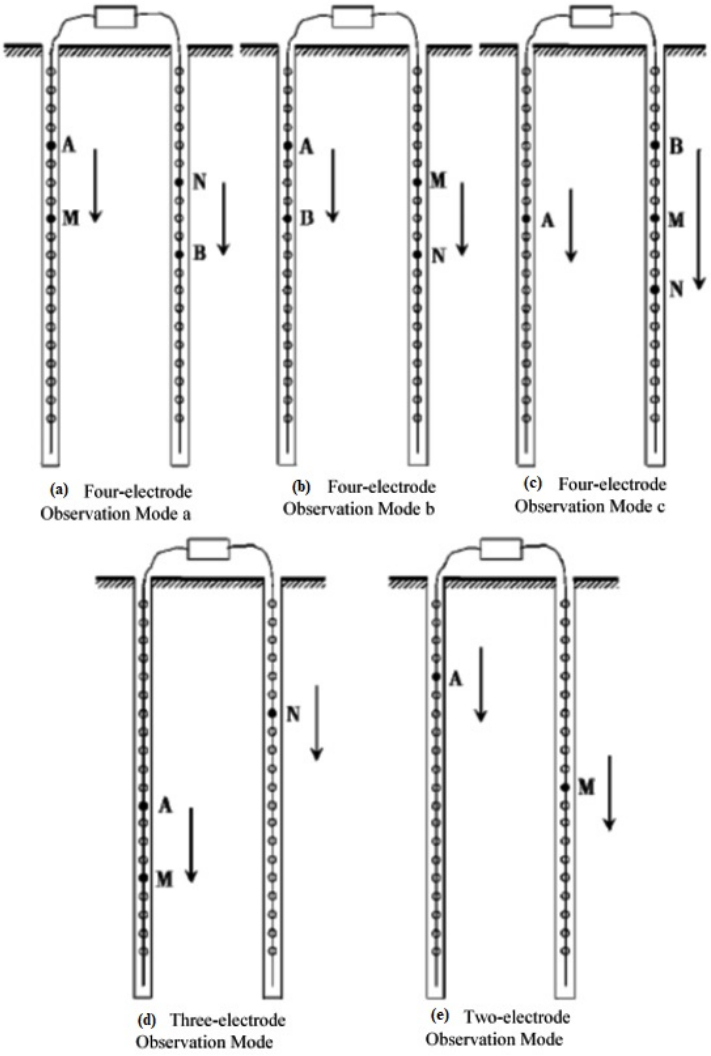

Figure 1. Conventional observation mode of cross-borehole resistivity CT [9]

Cross-borehole resistivity CT is a geophysical exploration method that involves placing electrodes into boreholes to collect formation resistivity data, commonly referred to internationally as Cross-borehole Electrical Resistivity Tomography. As shown in Figure 1 [9], multiple electrodes are arranged in the borehole during data acquisition for cross-borehole resistivity CT. A large amount of resistivity data is obtained by using different electrode combinations to improve data acquisition efficiency and data volume. The advantage of cross-borehole resistivity CT is that its electrodes are located in the borehole, closer to the surveyed area, thus providing higher resolution. Single cross-borehole resistivity CT exploration is often applied in advance geological forecasting and karst cave detection [10, 11]. In addition, cross-borehole resistivity CT technology has been widely used in monitoring geological carbon dioxide sequestration [12–14].

In this mode, A and B are transmitting electrodes that supply current underground; M and N are receiving electrodes that measure the potential difference between two points. Among them, the four-electrode observation mode (Type a), the three-electrode observation mode, and the two-electrode observation mode are the most typical and commonly used observation modes. In this study, Res2dmod software is used for forward numerical simulation, with 2% noise added to the numerical simulation results as synthetic data, which is then inverted in Res2dinv. The device type used in this study is the four-electrode observation mode (Type a).

The cross-hole resistivity method is a special form of the direct current resistivity method. The measurement mode of the direct current resistivity method is shown in Figure 2.

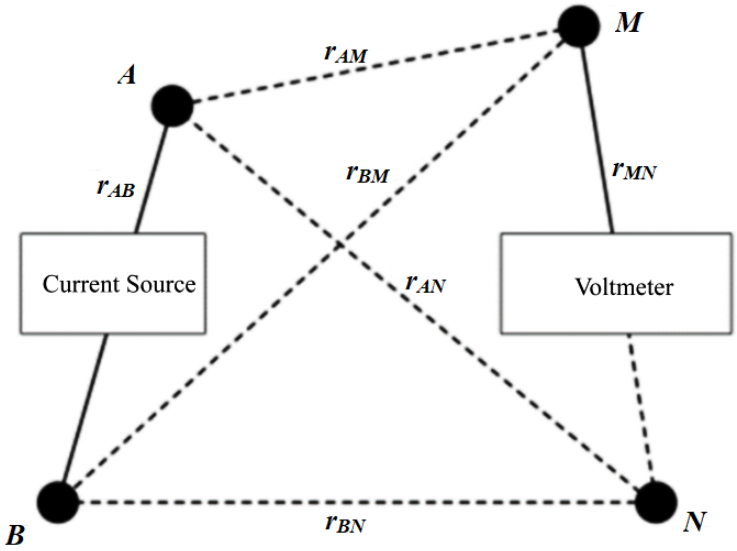

Figure 2. Schematic diagram of direct current resistivity method

Assuming there is a point current source in a homogeneous half-space underground, in this case, the current rapidly flows out from the current source radially, and the equipotential surface is distributed hemispherically. The supply current is perpendicular to the equipotential surface. At this time, the potential at any point P is:

$$u = \frac{\rho I}{2\pi r} \tag{1}$$

In the above equation: r is the distance from the electrode to point P (including the ground), in meters (m); ρ is the resistivity, in ohm-meters $(\Omega \cdot m)$; I is the supply current intensity, in amperes (A); u is the potential, in volts (V). From the above equation, it can be seen that the potential at each point on the hemispherical surface with radius r is the same. The calculation formula for underground resistivity is referred to as Eq. (2).

$$\rho = \frac{2\pi}{\left(\frac{1}{r_{AM}} - \frac{1}{r_{BM}} - \frac{1}{r_{AN}} + \frac{1}{r_{BN}}\right)} \frac{\Delta u_{MN}}{I} = K \frac{\Delta u_{MN}}{I} \tag{2}$$

where,

$$K = \frac{2\pi}{\left(\frac{1}{r_{AM}} - \frac{1}{r_{BM}} - \frac{1}{r_{AN}} + \frac{1}{r_{BN}}\right)} \tag{3}$$

K is called the configuration coefficient, r_{AM} is the distance between A and M, r_{BM} is the distance between B and M, r_{AN} is the distance between A and N, r_{BN} is the distance between B and N, Δu_{MN} is the potential

difference between M and N, and I is the supply current intensity. When the positions of all electrodes remain unchanged, K is a constant. Since the configuration coefficient K is known, the formation resistivity ρ can be calculated as long as the current intensity and voltage between two points are measured. The above formula is only applicable to homogeneous half-space media. When the distribution of electrical properties of underground rocks is non-uniform (with two or more rocks or ores with different conductivities) or when the surface is uneven, the resistivity calculated by the method and formula for determining the resistivity of a homogeneous horizontal earth is called apparent resistivity, denoted by ρ_s, with the same units as resistivity.

Numerical simulation consists of two steps: forward and inversion. The input data for forward simulation are observation parameters and model resistivity parameters, and the obtained data are underground apparent resistivity distribution data. In actual exploration, the collected data are underground apparent resistivity distribution data. The apparent resistivity data reflect the underground electrical structure, which is generally rough and requires inversion processing to obtain the true underground electrical structure. Therefore, in resistivity numerical simulation, noise needs to be added to the forward results to obtain synthetic data, and inversion interpretation of synthetic data is performed to discuss the exploration effect of the research content.

In this study, Res2dmod was used for forward modeling. Res2dmod is a numerical modeling software developed by AGS that can be used for 2D direct current resistivity modeling. Its data format is simple and clear, and it has a graphical user interface, greatly facilitating numerical simulation work for users. The inversion software is Res2dinv, which is a data processing software for direct current resistivity methods developed by AGS. The interface is simple, allowing for the setting of multiple inversion parameters and offering powerful functions. Random noise was added to the numerical simulation results of Res2dmod to obtain synthetic data, which was interpreted by inversion using Res2dinv to preliminarily analyze the application effect of the research content in actual exploration. Both software can support the finite difference method, which was used for numerical simulation work in this study.

The basic idea of finite difference numerical simulation is to discretize the region to be solved into multiple rectangular grids, represent the spatial distribution of the electric field with the parameter values at the center nodes of the grids, and replace the partial derivatives of the potential function with difference quotients at each grid center node. This discretizes the equation into a difference format, ultimately forming a linear system of equations regarding the potentials at the grid center nodes. Solving the system of equations yields the numerical solutions at each node. Therefore, the finite difference forward calculation for the direct current method can generally be divided into three steps: grid subdivision, constructing difference equations, and solving the linear equations. The finite difference method is flexible, simple, highly versatile, and easy to implement on computers. In Res2dmod, the 2-D model using the finite difference method divides the subsurface into multiple blocks using rectangular grids (see Figure 3). The finite difference method determines the potential at the nodes of the rectangular grids, which consist of N nodes in the horizontal direction and M nodes in the vertical direction.

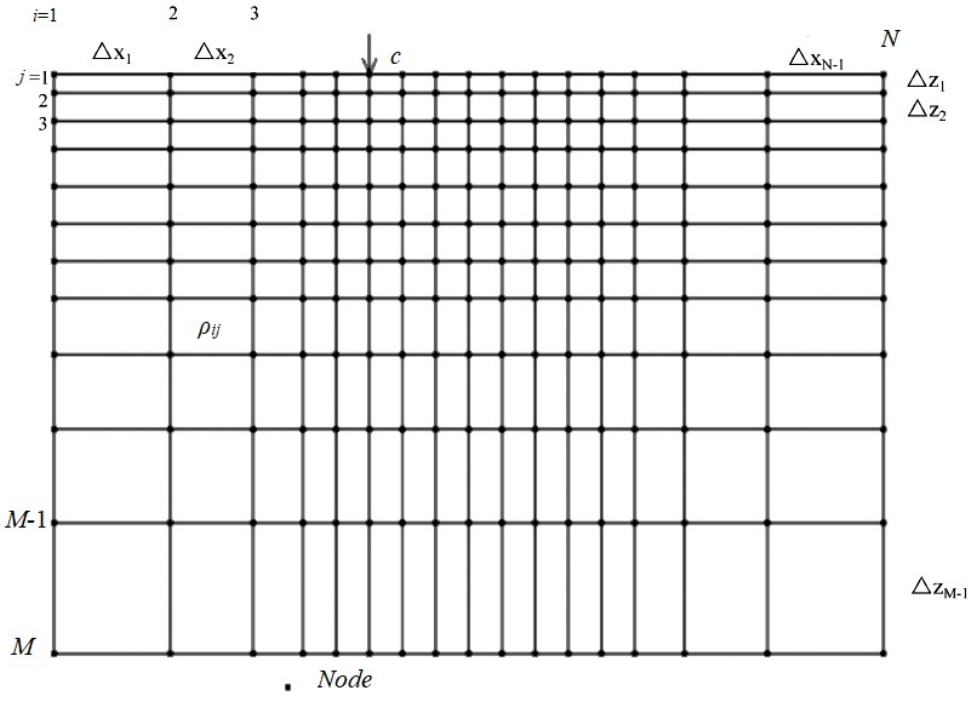

Figure 3. Schematic diagram of finite difference grid

The basic idea of inversion is to set an initial model, read the observation parameters of the actual data, calculate the apparent resistivity parameters generated by the model, and compare them with the actual data. Finally, the Root Mean Square Error (RMSE) is calculated to assess the degree of difference between the inversion model and the actual formation, which constitutes one round of inversion. After the first round of inversion, a model that fits the actual data more closely is calculated based on the inversion parameter information; this is the subsequent inversion mode. When the RMSE is reduced to a certain value, the inversion is considered converged, and the model calculation is stopped. The inversion method of Res2dinv is based on the smoothness-constrained least squares method, and the equation for the smoothness-constrained least squares method is as follows:

$$\left(\mathbf{J}^{\mathrm{T}}\mathbf{J}+\lambda\mathbf{F}\right)\Delta\mathbf{q}_{\mathrm{k}}=\mathbf{J}^{\mathrm{T}}\mathbf{g}-\lambda\mathbf{F}\mathbf{q}_{\mathrm{k}-1} \tag{4}$$

where,

$$\mathbf{F}=\alpha_X\mathbf{C}^{\mathrm{T}}{}_{\mathrm{X}}\mathbf{C}_{\mathrm{x}}+\alpha_Z\mathbf{C}^{\mathrm{T}}{}_{\mathrm{z}}\mathbf{C}_{\mathrm{z}} \tag{5}$$

C_x is the horizontal roughness filter, C_Z is the vertical roughness filter, J is the Jacobian matrix of partial derivatives, J^T is the transpose of J, λ is the damping coefficient, q is the model vector, g is the data error vector, α_X is the weight of the horizontal roughness filter, α_Z is the weight of the vertical roughness filter, and k denotes the number of inversion iterations.

In this modeling, the number of constructed grids will be specified; the more grids there are, the higher the refinement of the model. Additionally, the RMSE of the inversion will be indicated; a smaller RMSE implies a higher similarity between the inversion model and the real model, generally below 3%, to ensure the accuracy of the numerical simulation results.

3 Model Construction and Observation Parameter Settings

During the construction of cutoff walls, due to the differences in construction materials, the resistivity of the cutoff walls may vary. Currently, the most widely used types in China are plastic concrete walls and reinforced concrete walls, and in some scenarios, clay concrete walls and ordinary concrete walls are also applied. The resistivity of these types of continuous walls is shown in Table 1 [15, 16].

Table 1. Types of concrete walls and their resistivity

Type of Concrete Wall	Resistivity (Ω·m)
Ordinary Concrete Wall	104 ~ 109
Reinforced Concrete Wall	470 ~ 530
Clay Concrete Wall	100 ~ 400
Plastic Concrete Wall	130 ~ 1000

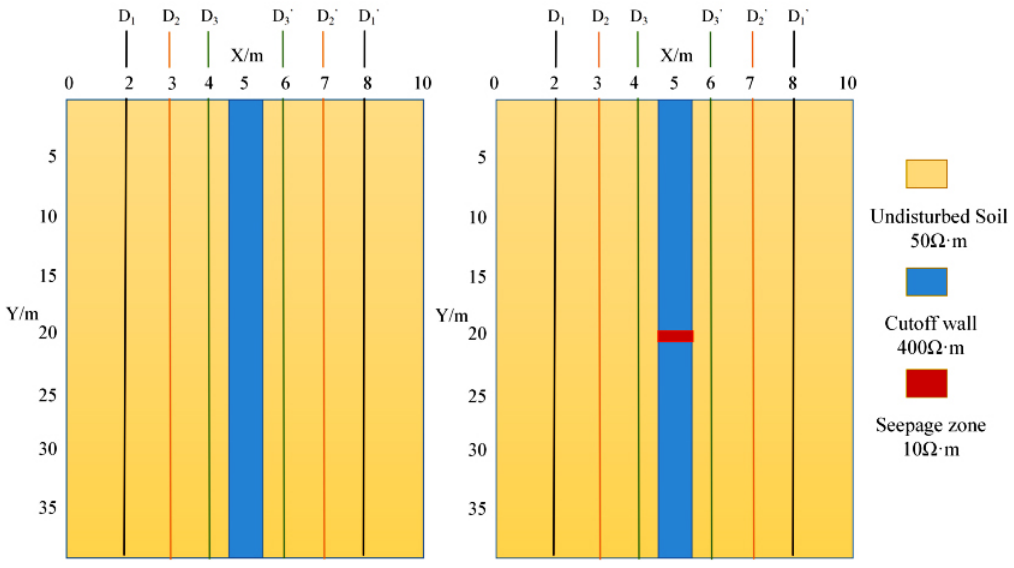

Figure 4. Schematic diagram of resistivity model

During the construction of cutoff walls, the surrounding rock is usually Quaternary soil, with a resistivity ranging from 30 to 70 $\Omega \cdot \mathrm{m}$. Currently, the main method for detecting cutoff walls based on underground resistivity characteristics is the high-density electrical method. Qi and Yan [17] used the high-density electrical method to detect dam cutoff walls and achieved good results in assessing both the dam foundation quality and the cutoff wall quality. Al-Fares [18] utilized resistivity imaging to detect a dam cutoff wall in Syria, proving the effectiveness of this method. Summarizing the resistivity change characteristics of cutoff wall leakage, it is known that after leakage occurs in a cutoff wall, the water saturation in the leakage area increases, and the resistivity decreases [19, 20]. Analyzing low-resistivity anomaly characteristics will help practitioners determine the seepage range.

Based on the above electrical characteristics, to study the impact of borehole spacing on detection results, this paper set borehole spacings of 6m, 4m, and 2m, constructing the resistivity model shown in Figure 4.

In the figure, D_1D_1', D_2D_2', and D_3D_3' represent three pairs of boreholes. The yellow area represents undisturbed soil with a resistivity of 50 $\Omega \cdot \mathrm{m}$, the blue area represents the cutoff wall with a resistivity of 400 $\Omega \cdot \mathrm{m}$, and the red area represents the seepage area with a resistivity of 10 $\Omega \cdot \mathrm{m}$.

4 Results Presentation

In the numerical simulation, the number of electrodes per borehole is set to 30, with a total of 60 electrodes and a borehole spacing of 2m. The model's horizontal range is 10m, and the vertical range is 35m. The finite difference forward model consists of 70 vertical grids and 400 horizontal grids, totaling 28,000 grids. The inversion RMSE converges to below 1%, and the numerical simulation results are shown in Figure 5.

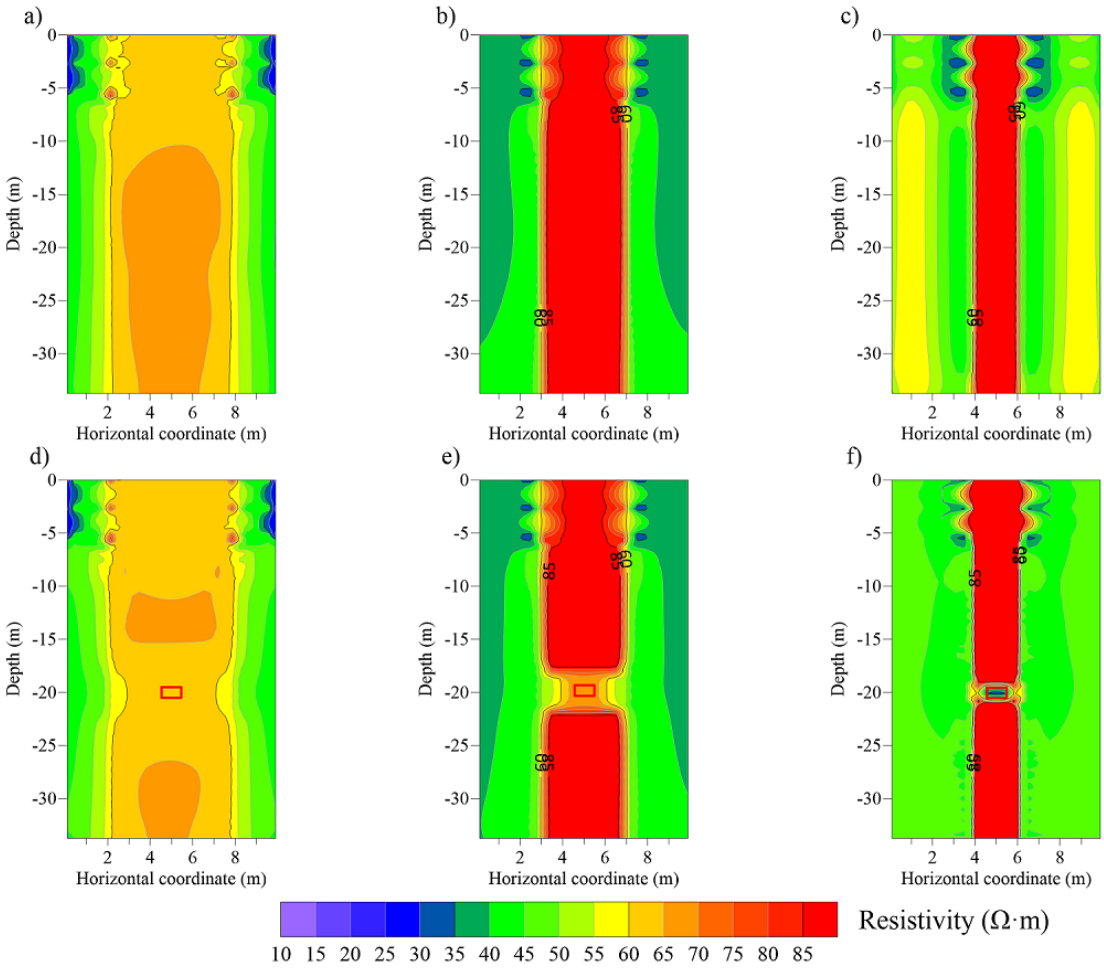

Figure 5. Inversion of synthetic data

In Figure 5, subgraphs (a), (b), and (c) display the resistivity distribution cross-sections with borehole spacings of 6m, 4m, and 2m, respectively, before seepage occurs. Subgraph (d), subgraph (e) and subgraph (f) show the resistivity distribution cross-sections with borehole spacings of 6m, 4m, and 2m, respectively, after seepage occurs.

From the numerical simulation results, it can be seen that after seepage occurs in the concrete wall, the resistivity contour lines tend to concave toward the seepage area. The clarity of the seepage area boundary increases as the

borehole spacing decreases, and the inverted resistivity values are closer to the values of the true model. The detection effect is best when the borehole spacing is 2m, accurately determining the seepage area.

To quantify the simulation results, Table 2 shows the maximum, minimum, and average resistivity values in the cutoff wall region with horizontal coordinates between 4.5m and 5.5m after seepage occurs.

Table 2. Resistivity statistics of cutoff wall region after seepage

Borehole Spacing (m)	Maximum Resistivity (Ω·m)	Minimum Resistivity (Ω·m)	Average Resistivity (Ω·m)
6	66.49	63.43	65.62
4	97.90	66.80	91.78
2	259.10	36.74	224.86

As shown in Table 2, when the borehole spacing decreases, the maximum and average resistivity values representing the cutoff wall resistivity increase, showing a higher similarity to the resistivity of the forward model. The difference between the minimum and maximum resistivity values increases, indicating a greater distinction between seepage and non-seepage areas, leading to better cross-hole resistivity detection results.

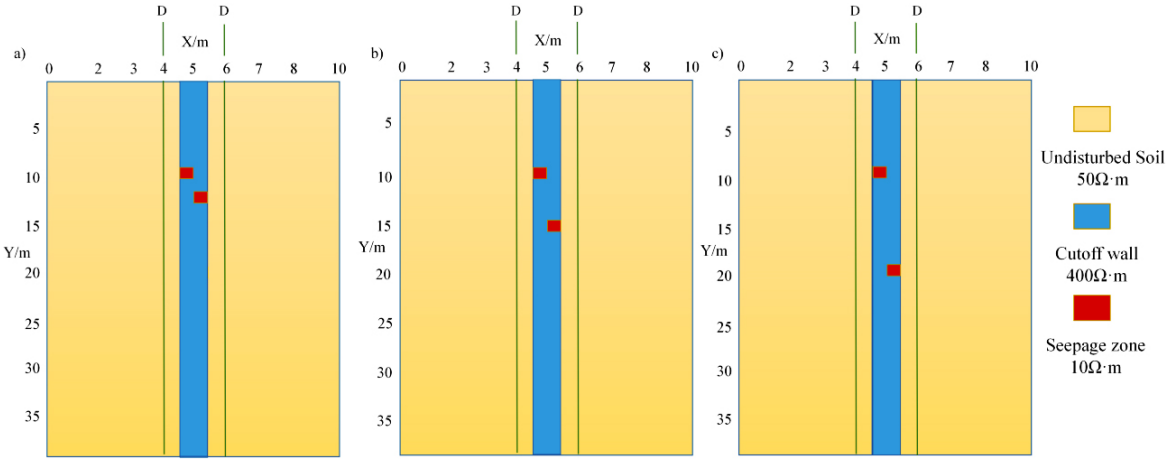

Figure 6. Two-point seepage model diagram

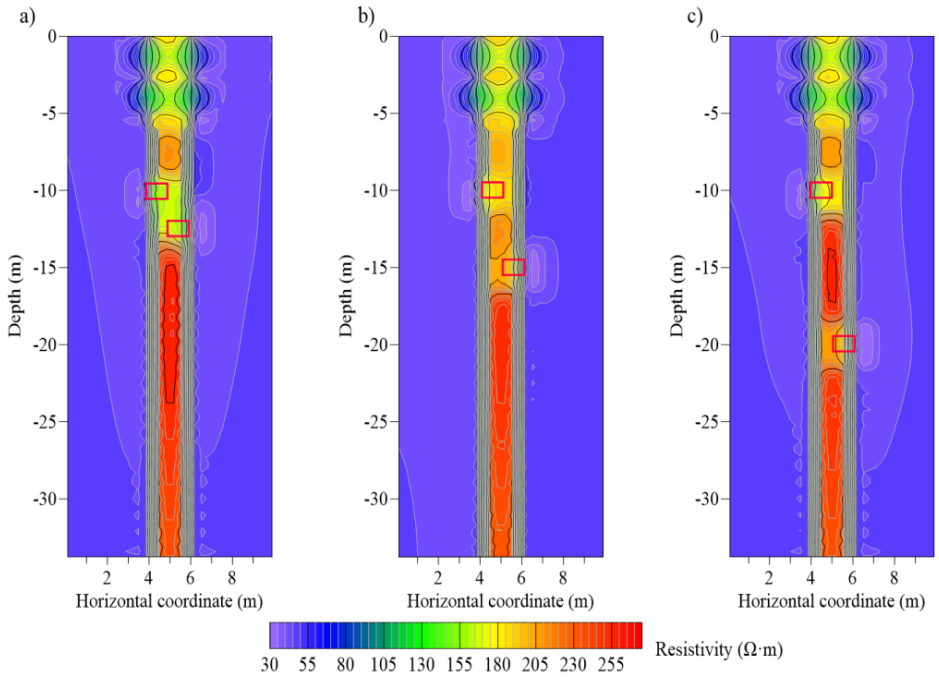

Figure 7. Two-point seepage results diagram

Cutoff walls may have multiple seepage points. Due to resolution limitations, conventional ground detection methods cannot separate multiple seepage areas from superimposed anomalies. To further discuss the detection effect of multiple seepage points, this paper designs a cross-borehole resistivity CT model with a borehole spacing of 2m, as shown in Figure 6. Two seepage points are set, and subgraph (a), subgraph (b) and subgraph (c) of Figure 6 represent the cases where the distance between the two seepage points is 2.5m, 5m, and 10m, respectively. The inversion RMSE of the numerical simulation converges to below 1%, and the results are shown in Figure 6.

Subgraph (a), subgraph (b) and subgraph (c) of Figure 7 represent the results for seepage point spacings of 2.5m, 5m, and 10m, respectively. Comparing the three results, it is evident that when the seepage point spacing is 10m, under the simulation conditions of this study, the cross-borehole resistivity CT method effectively distinguishes the low-resistivity anomalies generated by the two seepage areas. When the seepage point spacing is 5m, the location of the seepage points can be qualitatively determined based on the trend of the contour lines, and the cross-borehole resistivity CT method achieves a relatively satisfactory differentiation. When the seepage point spacing is 2.5m, the two low-resistivity areas influence each other, and under the simulation conditions of this study, the cross-borehole resistivity CT method cannot effectively identify the two seepage points.

5 Conclusion and Outlook

Based on the analysis of the simulation results, the following conclusions can be drawn:

(1) Cross-borehole resistivity CT has a certain effectiveness in detecting seepage in concrete cutoff walls, capable of distinguishing the depth range of seepage. The smaller the spacing between cross-holes, the more accurate the delineation of the seepage area, resulting in more precise results. However, reducing the cross-hole spacing decreases the detection range, and large-scale detection would increase costs. In actual detection, the optimal borehole spacing should be determined based on the site conditions.

(2) When there are multiple seepage points, the resolution of cross-borehole resistivity CT is somewhat limited. Under the conditions of this study, the cross-borehole resistivity CT method cannot distinguish two seepage points with a vertical distance of 2.5m. In actual detection, if a low-resistivity anomaly region with a wide vertical distribution is found, detection parameters should be adjusted or other data processing methods should be used for further analysis.

(3) The premise of this simulation is that each underground electrode is well-grounded, capable of stably supplying current underground and measuring potential under ideal conditions. In actual engineering, there may be cases where some measurement points have distorted signals, which could affect detection results.

(4) The inversion method used in this study is the smoothness-constrained least squares method, which does not achieve ideal inversion results for the two-seepage model. In future research, other inversion methods will be attempted to improve the differentiation of multiple seepage areas.

(5) The advantage of cross-borehole resistivity CT lies in its accurate detection results and higher resolution for deep engineering structure detection. However, its disadvantages include a small detection range and high cost. In practical applications, targeted fine detection should be carried out in certain areas after understanding the approximate distribution of defects.

(6) The application of cross-borehole resistivity CT in engineering can evolve from single-time detection to sustainable monitoring, ensuring the safe operation of key parts of the project. Since the electrodes corrode and rust during use, applying this method for monitoring poses a greater challenge to electrode manufacturing processes.

Data Availability

The data used to support the findings of this study are available from the corresponding author upon request.

Conflicts of Interest

The authors declare that they have no conflicts of interest.

References

[1] W. F. Xu and Y. Zhou, "Testing study of plastic concrete cutoff wall impermeability," *Yellow River*, vol. 35, no. 7, pp. 89–91, 2013. https://doi.org/10.3969/j.issn.1000-1379.2013.07.031

[2] K. B. Deng, "Application analysis of several non-destructive testing techniques in quality testing of impermeable walls," *Adv. Sci. Technol. Water Resour.*, vol. 27, no. 2, pp. 50–54, 2007. https://doi.org/10.3880/j.issn.1006-7647.2007.02.013

[3] H. Q. Li, Y. G. Xu, F. P. Gan, W. Zhao, and J. J. Lu, "Application of cross-well electromagnetic wave CT technique to evaluating weathered igneous rock dam structure of Zuojiang river power station," *Rock Soil Mech.*, vol. 31, no. z1, pp. 430–434, 2010. https://doi.org/10.3969/j.issn.1000-7598.2010.z1.068

[4] D. K. Cao, J. J. Shang, and S. B. Chen, "Application of comprehensive CT non-destructive testing technology on the seepage control wall of the Qianping reservoir dam foundation," *China Water Resour.*, vol. 2020, no. 18, pp. 61–62, 2020. https://doi.org/10.3969/j.issn.1000-1123.2020.18.029

[5] H. Shima and T. Sakayama, "Resistivity tomography: An approach to 2-D resistivity inverse problems," *SEG Tech. Prog. Exp. Abstr.*, pp. 59–61, 1987. https://doi.org/10.1190/1.1892038

[6] W. Daily and E. Owen, "Cross-borehole resistivity tomography," *Geophys.*, vol. 56, no. 8, pp. 1228–1235, 1991. https://doi.org/10.1190/1.1443142

[7] L. W. Chai, G. Y. Tang, G. Q. Wang, and Y. P. Hu, "Application of ultra-high density cross-hole resistivity imaging in the detection of bored pile depth," *Chin. J. Eng. Geophys.*, vol. 18, no. 2, pp. 252–256, 2021. https://doi.org/10.3969/j.issn.1672-7940.2021.02.014

[8] Y. C. Ou, F. P. Hu, and L. Tan, "Study on multi-hole resistivity combined imaging technology of karst hidden dangers in urban subway," *J. Saf. Sci. Technol.*, vol. 17, no. 4, pp. 141–146, 2021. https://doi.org/10.11731/j.issn.1673-193x.2021.04.023

[9] S. C. Li, Z. Y. Liu, B. Liu, X. J. Xu, C. W. Wang, L. C. Nie, H. F. Sun, J. Song, and S. R. Wang, "Boulder detection method for metro shield zones based on cross-hole resistivity tomography and its physical model tests," *Chin. J. Geotech. Eng.*, vol. 37, no. 3, pp. 446–457, 2015.

[10] S. Liang, J. H. Chen, H. T. Li, W. L. Luo, Y. Z. Luo, J. J. Ai, and W. Liao, "Detection of karst caves using the cross-hole resistivity method based on the squirrel search algorithm," *Geophys. Geochem. Explor.*, vol. 46, no. 5, pp. 1296–1305, 2022. https://doi.org/10.11720/wtyht.2022.1262

[11] N. B. Li, Y. H. Zhang, L. C. Nie, Z. Y. Liu, L. Yang, and Z. Dong, "Study in 3D cross-hole resistivity ahead prospecting method in tunnel and its field application," *J. Basic Sci. Eng.*, vol. 29, no. 5, pp. 1140–1155, 2021. https://doi.org/10.16058/j.issn.1005-0930.2021.05.006

[12] F. M. Wagner, T. Günther, C. Schmidt-Hattenberger, and H. Maurer, "Constructive optimization of electrode locations for target-focused resistivity monitoring," *Geophysics*, vol. 80, no. 2, pp. E29–E40, 2015. https://doi.org/10.1190/geo2014-0214.1

[13] P. Bergmann, M. Diersch, J. Götz, M. Ivandic, A. Ivanova, C. Juhlin, and F. Zhang, "Review on geophysical monitoring of CO2 injection at Ketzin, Germany," *J. Petrol. Sci. Eng.*, vol. 139, pp. 112–136, 2016. https://doi.org/10.1016/j.petrol.2015.12.007

[14] P. Bergmann, C. Schmidt-Hattenberger, D. Kiessling, C. Rücker, T. Labitzke, J. Henninges, and H. Schütt, "Surface-downhole electrical resistivity tomography applied to monitoring of CO2 storage at Ketzin, Germany," *Geophysics*, vol. 77, no. 6, pp. B253–B267, 2012. https://doi.org/10.1190/geo2011-0515.1

[15] H. J. Li, Y. J. Xie, Z. L. Yi, Y. B. Tan, Z. W. Feng, B. Fang, and L. Yang, "Advance in research on electrical resistivity of concrete," *Concrete*, vol. 2011, no. 6, pp. 35–40, 2011. https://doi.org/10.3969/j.issn.1002-3550.2011.06.011

[16] Z. Y. Liu and Z. F. Zhan, "Research on electrical resistivity of concrete and its application in durability appreciation of reinforced concrete," *Concrete*, vol. 2006, no. 10, pp. 13–16, 2006. https://doi.org/10.3969/j.issn.1002-3550.2006.10.005

[17] M. X. Qi and J. M. Yan, "Application of high-density electric survey in reservoir dam foundation nondestructive testing," *Coal Geol. China*, vol. 21, no. 10, pp. 54–56, 2010. https://doi.org/10.3969/j.issn.1674-1803.2009.10.015

[18] W. Al-Fares, "Contribution of the geophysical methods in characterizing the water leakage in Afamia B dam, Syria," *J. Appl. Geophys.*, vol. 75, no. 3, pp. 464–471, 2011. https://doi.org/10.1016/j.jappgeo.2011.07.014

[19] G. X. Guo, B. D. Xin, and W. C. Liu, "The application of electric sounding in investigation of Zhangfang-emergency karst wellfield, NW-Beijing," *Geophys. Geochem. Explor.*, vol. 34, no. 2, pp. 225–228, 2010.

[20] Y. Q. Liu, H. M. Xu, and J. J. Hu, "Application of comprehensive geophysical exploration technique to detecting hidden defects of reservoir dams," *Chin. J. Eng. Geophys.*, vol. 16, no. 4, pp. 546–551, 2019. https://doi.org/10.3969/j.issn.1672-7940.2019.04.018